

06.5

## Defining of optimal model of interaction of hydrogen atom with platinum nanoparticle on graphene surface using quantum-mechanical calculations

© S.A. Smirnov<sup>1</sup>, D.D. Spasov<sup>1</sup>, R.M. Mensharapov<sup>2</sup>, S.A. Grigoriev<sup>1,3</sup>

<sup>1</sup> National Research University „Moscow Power Engineering Institute“, Moscow, Russia

<sup>2</sup> National Research Center „Kurchatov Institute“, Moscow, Russia

<sup>3</sup> North-West University, Potchefstroom, South Africa

E-mail: GrigoryevSA@mpei.ru

Received May 2, 2023

Revised October 20, 2023

Accepted October 20, 2023

The interaction of the surface of the support (graphene) and the Pt<sub>3</sub> nanocluster to which the hydrogen atom is adsorbed is considered. Two configurations of the initial position of the hydrogen atom have been studied: near the surface of graphene (the angle H–Pt–C is 90°) and at a distance from the surface of graphene (the angle H–Pt–C is 180°). The calculations were carried out using the Gaussian16 software package. For the first time, the geometries were optimized and compared for the two proposed models, the electron density was calculated using an SCF matrix, UV-visible spectra were built, consistent with experimental data. The obtained data confirm that when adsorbing hydrogen on active platinum centers located near the graphene surface, the hydrogen atom is preferably located in close proximity to the graphene surface.

**Keywords:** quantum mechanical calculations, hydrogen adsorption on a platinum electrocatalyst, graphene, structure of coronene, time-dependent density functional theory.

DOI: 10.61011/TPL.2024.01.57836.19613

Of particular importance for the development of modern electro-catalysts for fuel cells is the problem of determining the adsorption energy of hydrogen on the surface of active centers. The type of carbon carrier and crystal structure of platinum nanoparticles are known to influence the hydrogen adsorption energy [1,2]. There are various works that estimate adsorption energy values on different electric catalysts [3], including platinum electric catalysts on carbon carrier [4,5]. One of the promising carriers for platinum electric catalysts are graphene and graphene-like nanomaterials. Due to the high stability, specific conductivity and developed surface of such carriers, it is possible to significantly reduce the content of precious metal in the electric catalyst composition without deteriorating its activity and stability. Therefore, it is particularly important to evaluate the effect of the presence of this carrier on the hydrogen adsorption process on platinum nanoparticles during the hydrogen oxidation reaction. In [6,7], the interaction of proton with platinum nanoclusters has been considered, but the effect of the geometry of the adsorbed proton on the stability of graphene–platinum–proton systems has not been evaluated. The density functional theory (DFT) method can be used to calculate the electron density parameters and identify the regions of inhomogeneity of electron density surfaces [8,9]. Time-dependent density functional theory (TDDFT) [10] was used to calculate the UV-visible spectra of metal complexes, including platinum complexes. In this case, the problem of determining the model of hydrogen interaction with the lowest reaction energy with the surface of a platinum nanoparticle located on the surface of a nanostructured carbon carrier —

graphene, requires detailed consideration using the described methods.

To investigate the influence of the presence of carbon carrier on the mechanism of hydrogen adsorption on platinum nanoparticle, we considered two systems: hydrogen atom adsorbed on platinum nanocluster near the graphene surface (angle H–Pt–C is equal to 90°) and at a distance from the graphene surface (angle H–Pt–C is equal to 180°). The nanocluster within this model consists of three platinum atoms (Pt<sub>3</sub>) and is located above the surface of the coronene structure, which in this case acts as a model section of the graphene [11] surface. The hydrogen atom was attached to the nanocluster Pt<sub>3</sub> with the bond angle H–Pt–C equal to 90° (the hydrogen platinum bond is parallel to the plane in which the coronene structure lies) (Fig. 1, *a*, position *End*), and with the bond angle H–Pt–C equal to 180° (hydrogen–platinum bond is perpendicular to the plane in which the coronene structure lies) (Fig. 1, *b*, position *End*). Such systems exhibit different adsorption mechanisms: the system with an angle H–Pt–C equal to 90° demonstrates hydrogen adsorption directly near the surface, while the system with an angle H–Pt–C equal to 180° reproduces the possibility of hydrogen adsorption in the absence of significant interaction between hydrogen and the carrier surface, such as at the top of a platinum nanoparticle. Geometry optimization and calculation of UV-visible spectra were performed for these states. The geometry optimization was performed using the DFT method with the search for the ground state of the minimum energy of the system. UV-visible spectra were calculated using the TDDFT method. All calculations were performed

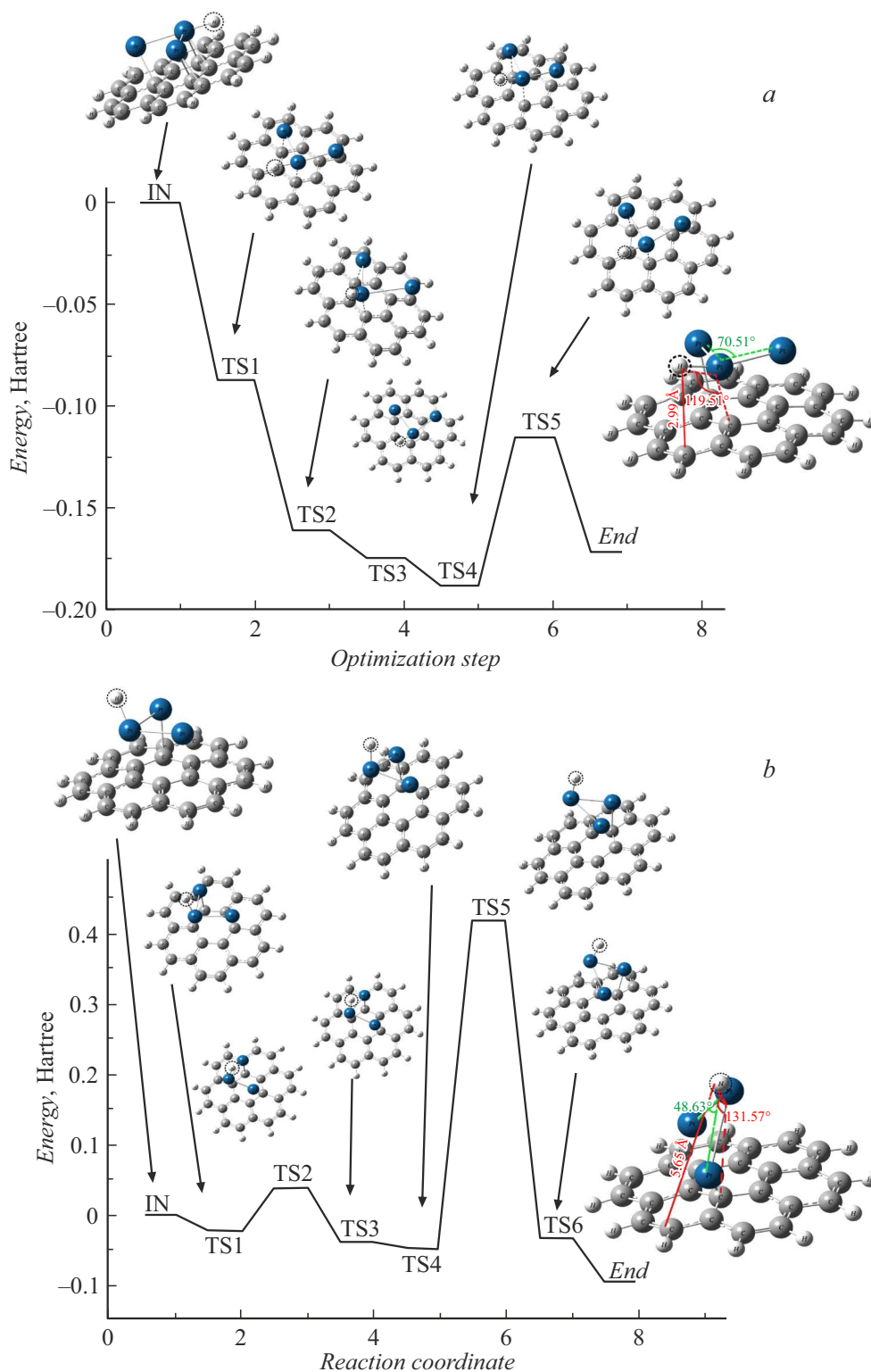


**Figure 1.** *a* — optimization steps for the system with hydrogen not forming an angle with the surface; *b* — optimization steps for the model geometry with hydrogen forming an angle with the surface.

in the Gaussian16 [12] software package. The model was decomposed by the ONIOM [13,14] method into two levels:

— the level of higher precision calculations was chosen for platinum atoms, the B3LYB functional with the

LANL2DZ basis (consisting of two parts: one part is a set of small compressed Gaussian functions and the other part is a set of larger fuzzy Gaussian functions) [15,16] was used;

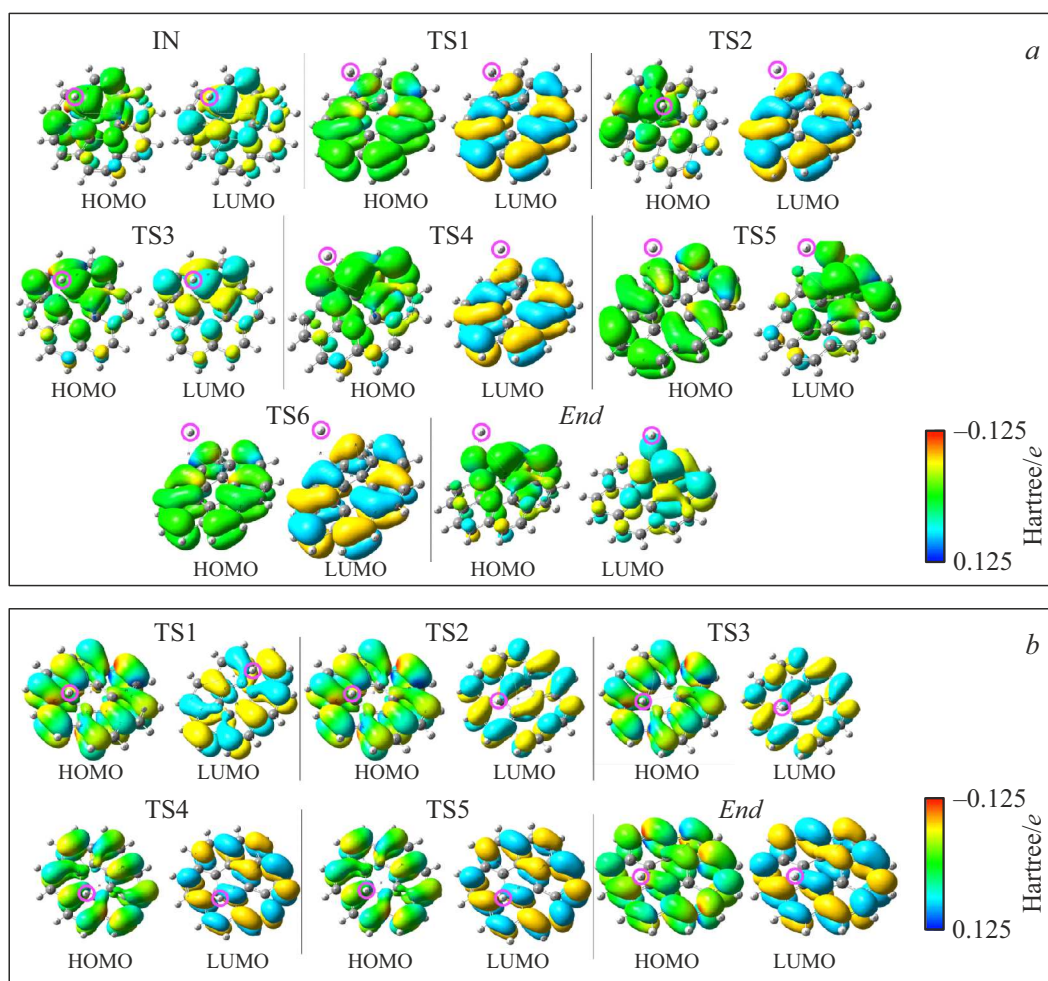


**Figure 2.** Change in electron density for different geometry optimization steps (adsorbed hydrogen atom circled). *a* — for a model with an angle H–Pt–C, equal to  $180^\circ$ ; *b* — for a model geometry with an angle H–Pt–C, equal to  $90^\circ$ .

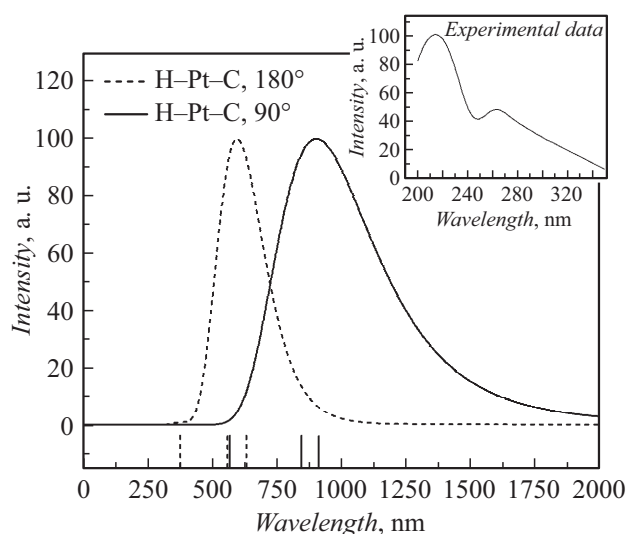
— the level of reduced detail was chosen for hydrogen and carbon atoms, and the B3LYB functional with the 631+G basis (including basis functions for valence electrons and additional polarization functions to account for correlation effects) [13] was used.

Fig. 1, *a* shows the change in the geometry of the system with angle H–Pt–C equal to  $90^\circ$  during its optimization: position IN — the geometry of the system at the calculation initialization, TS — the transitional states *End* — the final geometry of the system. The angle between the hydrogen atom and the platinum nanocluster changed as a result of the optimization was  $119.51^\circ$  for the *End* position; the interatomic distances in the coronene structure also changed (multiple bonds cease to exist for the central benzene ring), indicating that this system is stable, and the coronene structure affects both the platinum particle and the hydrogen attached to the platinum.

Figure 2, *b* shows the change in the electrostatic potential map for HOMO (highest occupied molecular orbital — highest occupied molecular orbital) and LUMO (lowest unoccupied molecular orbital — lowest valence molecular

orbital) during the geometry optimization process for a model with an angle H–Pt–C equal to  $90^\circ$ . HOMO and LUMO electron densities were constructed for the geometry of the system at each optimization step; the electron density from the self-consistent field (SCF) matrix was used to construct the molecular orbitals. The whole system has the same spin and positive charge (singlet state). From the analysis of electron density homogeneity we can conclude that such a system is well bound, and from the localization analysis we can speak about insignificant change of charge distribution over the system at optimization of geometry (position *End*). Insignificant changes in the spatial arrangement of the electron density indicate a weak change in the geometry of the system during the optimization, i.e. seven optimization steps are sufficient for good energy matching (the normalized gradient is  $5 \cdot 10^{-3}$  Hartree/Bohr).

Fig. 1, *b* shows the optimization steps of the model geometry, which was obtained by optimizing the initial configuration with the bond angle H–Pt–C equal to  $180^\circ$ . As can be seen from the geometry, the system is less stable as the hydrogen platinum nanocluster is removed from the



**Figure 3.** Calculated spectra for models with angle H–Pt–C, equal to  $90^\circ$  (solid line) and  $180^\circ$  (dashed line). The insert shows the experimental spectrum of [17]. Vertical lines indicate the peaks of singlet states for the calculated spectra.

surface of the coronene structure during the optimization; the angle between the surface and the hydrogen atom has changed to  $131.57^\circ$ .

The Pt–C distance for the model with the angle H–Pt–C equal to  $90^\circ$  is  $1.65 \text{ \AA}$ , indicating a strong covalent bond between the platinum and graphene atoms, while for the model with the angle H–Pt–C equal to  $180^\circ$  a change in the bond length of Pt–C to  $4.27 \text{ \AA}$  is observed for the platinum atom to which hydrogen is attached, indicating that there is no bonding between the platinum atom and the graphene surface.

Fig. 2, *a* shows the variation of the electrostatic potential map for HOMO and LUMO for the model with the H–Pt–C angle equal to  $180^\circ$ . Electron density dislocation is clearly visible: separately on platinum atoms and separately on graphene. The charge is distributed extremely unevenly: in the platinum–carbon region, a locally positive charge for the LUMO and HOMO orbitals is observed, shifted to the hydrogen atom. Analyzing the previously obtained results, we can state that the model with the angle H–Pt–C equal to  $90^\circ$ , has more homogeneous molecular orbitals for each of the geometry optimization the angle H–Pt–C equal to  $180^\circ$ .

The obtained calculated spectra in the UV-visible range and experimental data are presented in Fig. 3. The calculated spectrum for the model with the coupling angle H–Pt–C equal to  $90^\circ$ , agrees better with the experimental data due to the larger spectrum extent than the system with the coupling angle H–Pt–C equal to  $180^\circ$ . Comparing the experimental data [17] with the calculated data for the UV-visible spectrum, the following can be stated:

— hydrogen on the platinum surface is present in close proximity to the graphene surface;

— the platinum nanocluster is strongly bound to the graphene surface.

Thus, the hydrogen system with a bond angle H–Pt–C equal to  $90^\circ$  shows greater stability than the system with a bond angle H–Pt–C equal to  $180^\circ$ . This is evidenced by the geometry of the calculated systems: for the system with an angle H–Pt–C equal to  $180^\circ$ , the platinum with hydrogen is at a distance, i.e. dissociates while the system with an angle H–Pt–C equal to  $90^\circ$  is near the graphene surface. The highest convergence with experimental data on the UV-visible spectrum is provided by a system with a coupling angle H–Pt–C equal to  $90^\circ$ . It is reasonable to consider hydrogen adsorption on active centers of platinum nanoparticles located near the carrier surface (graphene) in the approximation, according to which the hydrogen atom is located in close proximity to the graphene surface.

The obtained results, indicating, in particular, the modifying influence of graphene carrier on the properties of platinum nanoparticles during hydrogen adsorption, allow us to conclude that it is reasonable to carry out detailed quantum mechanical calculations of the hydrogen–platinum–graphene system: determination of the interaction energy of hydrogen with platinum, bond length, IR and UV-visible spectra. Such extended calculations, in turn, will make it possible to explain the difference in the hydrogen adsorption energies on the active centers of platinum electric catalysts based on different nanocarbon carriers, to increase their activity, stability, and the degree of platinum utilization.

## Funding

The work was carried out with the financial support of the Ministry of Science and Higher Education of the Russian Federation under the state task № FSWF-2023-0014 in the field of scientific activity for 2023–2025.

## Conflict of interest

The authors declare that they have no conflict of interest.

## References

- [1] R.M. Mensharapov, D.D. Spasov, N.A. Ivanova, A.A. Zasykina, S.A. Smirnov, S.A. Grigoriev, *Inorganics*, **11**, 103 (2023). DOI: 10.3390/inorganics11030103
- [2] H. Yan, H. Lv, H. Yi, W. Liu, Y. Xia, X. Huang, W. Huang, S. Wei, X. Wu, J. Lu, *J. Catal.*, **366**, 70 (2018). DOI: 10.1016/j.jcat.2018.07.033
- [3] X. Zhang, Z. Xia, H. Li, S. Yu, S. Wang, G. Sun, *RSC Adv.*, **9**, 7086 (2019). DOI: 10.1039/c9ra00167k
- [4] R. Habibpour, A. Ahmadi, M. Faghhihasiri, P. Amani, *Appl. Surf. Sci.*, **528**, 147043 (2020). DOI: 10.1016/j.apsusc.2020.147043
- [5] A.C. Reber, S.N. Khanna, *Acc. Chem. Res.*, **50**, 255 (2017). DOI: 10.1021/acs.accounts.6b00464

- [6] Y. Zhu, P. Tian, H. Jiang, J. Mu, L. Meng, X. Su, Y. Wang, Y. Lin, Y. Zhu, L. Song, H. Li, *CCS Chem.*, **3**, 2539 (2020). DOI: 10.31635/ccschem.020.202000497
- [7] M. Andersen, L. Hornekær, B. Hammer, *Phys. Rev. B*, **86**, 085405 (2012). DOI: 10.1103/PhysRevB.86.085405
- [8] L.F. Tsague, G.W. Ejuh, J.M.B. Ndjaka, *Opt. Quantum Electron.*, **54**, 621 (2022). DOI: 10.1007/s11082-022-03915-1
- [9] S. Zhang, B. Cheng, Z. Jia, X. Jin, Z. Zhao, G. Wu, *Adv. Composit. Hybrid Mater.*, **5**, 1658 (2022). DOI: 10.1007/s42114-022-00514-2
- [10] P. Jena, A.W. Catelman, Jr., *PNAS*, **103**, 10560 (2016). DOI: 10.1073/pnas.0601782103
- [11] S. Kumar, S. Sharma, R. Karmaker, D. Sinha, *Mater. Today Commun.*, **26**, 101755 (2021). DOI: 10.1016/j.mtcomm.2020.101755
- [12] M.J. Frisch, G.W. Trucks, H.B. Schlegel, G.E. Scuseria, M.A. Robb, J.R. Cheeseman, G. Scalmani, V. Barone, G.A. Petersson, H. Nakatsuji, X. Li, M. Caricato, A.V. Marenich, J. Bloino, B.G. Janesko, R. Gomperts, B. Mennucci, H.P. Hratchian, J.V. Ortiz, A.F. Izmaylov, J.L. Sonnenberg, D. Williams-Young, F. Ding, F. Lipparini, F. Egidi, J. Goings, B. Peng, A. Petrone, T. Henderson, D. Ranasinghe, V.G. Zakrzewski, J. Gao, N. Rega, G. Zheng, W. Liang, M. Hada, M. Ehara, K. Toyota, R. Fukuda, J. Hasegawa, M. Ishida, T. Nakajima, Y. Honda, O. Kitao, H. Nakai, T. Vreven, K. Throssell, J.A. Montgomery, J.E. Peralta, F. Ogliaro, M.J. Bearpark, J.J. Heyd, E.N. Brothers, K.N. Kudin, V.N. Staroverov, T.A. Keith, R. Kobayashi, J. Normand, K. Raghavachari, A.P. Rendell, J.C. Burant, S.S. Iyengar, J. Tomasi, M. Cossi, J.M. Millam, M. Klene, C. Adamo, R. Cammi, J.W. Ochterski, R.L. Martin, K. Morokuma, O. Farkas, J.B. Foresman, D.J. Fox, *Gaussian 16, Revision B.01* (Gaussian, Inc., Wallingford, 2016).
- [13] F. Jensen, *WIREs Comput. Mol. Sci.*, **3**, 273 (2013). DOI: 10.1002/wcms.1123
- [14] L.W. Chung, W.M.C. Sameera, R. Ramozzi, A.J. Page, M. Hatanaka, G.P. Petrova, T.V. Harris, X. Li, Z. Ke, F. Liu, H.-B. Li, L. Ding, K. Morokuma, *Chem. Rev.*, **115**, 5678 (2015). DOI: 10.1021/cr5004419
- [15] C. Garino, L. Salassa, *Phil. Trans. R. Soc. A*, **371**, 20120134 (2013). DOI: 10.1098/rsta.2012.0134
- [16] T.E.-M. Hosseinnejad, F.B. Fatemeh, *RSC Adv.*, **8**, 12232 (2018). DOI: 10.1039/c8ra00283e
- [17] E. Gharibshahi, E. Saion, *Int. J. Mol. Sci.*, **13**, 14723 (2012). DOI: 10.3390/ijms131114723

*Translated by J.Deineka*